Optical collection of extracellular vesicles in a culture medium enhanced by interactions with gold nanoparticles

Yumeki Tani · Kenta Ochiai · Takashi Kaneta*

Department of Chemistry, Okayama University, Okayama, 700-8530, Japan

* To whom correspondence should be addressed.

E-mail: kaneta@okayama-u.ac.jp

ORCID: 0000-0002-6004-7973 (Y. Tani)

0000-0001-9076-3906 (T. Kaneta)

Abstract

Extracellular vesicles (EVs) exist in biological fluids such as blood, urine, and cerebrospinal fluid and are promising cancer biomarkers. Attempts to isolate and analyze trace EVs, however, have been a challenge for researchers studying their functions and secretion mechanisms, which has stymied the options for diagnostic application. This study demonstrated a collection of EVs that was enhanced by gold nanoparticles (AuNPs) via the use of optical force. The collection system consists of an inverted microscope equipped with a CCD camera, a square capillary connected with a PTFE tube, and an Nd:YAG laser that generates optical force. The laser beam was focused on a capillary wall in which a cell culture medium containing EVs flowed continuously. Control of the surface charges on both the capillary wall and the AuNPs achieved the collection and retention of EVs on the capillary wall. The positively charged capillary wall retained EVs even after the laser irradiation was halted due to the negative charges inherent on the surface of EVs. Conversely, positively charged AuNPs had a strong electrostatic interaction with EVs and enhanced the optical force acting on them, which made collecting them a much more efficient process.

Introduction

Extracellular vesicles (EVs) is a generic term for particles naturally released from biological cells, as defined by the International Society for Extracellular Vesicles (ISEV) [1]. EVs are surrounded by lipid bilayers, cannot replicate from different living cells, exist in all types of bodily fluids such as blood [2], urine [3,4], and saliva [5], and circulate in the body to deliver their contents to other cells [6]. EVs are mainly classified as exosomes, microvesicles, and apoptotic bodies based on their intracellular origins. Exosomes, microvesicles, and apoptotic bodies generally range in the sizes of from 50-150 nm, 100-1,000 nm, and 1-4 μm, respectively. EV classification as either exosomes or microvesicles is roughly due to their biogenesis and secretion mechanisms, but the ISEV has not clearly discriminated the distinction because the components are similar and the size ranges overlap. In general, tetraspanins (CD9, CD63, CD81) abundantly exist on the membranes of exosomes, whereas integrins and CD40 are abundantly present on the membranes of microvesicles. Therefore, these proteins are frequently used as markers to detect the corresponding EVs.

Recently, many researchers have challenged the development of biosensors that integrate enrichment and detection systems for profiling exosomes [6]. These systems include fluorescence-integrated microfluidics biosensors [7], surface-enhanced Raman scattering (SERS)-based biosensors [8], electrochemistry-based biosensors [9], and field-effect transistor-based biosensors [10]. The fluorescence-integrated microfluidics biosensors integrate the channels to capture and detect exosomes using antibodies of exosomal membrane proteins. The SERS-based biosensors mainly include two types of biosensors: label-free and tag-based platforms. The label-free platforms have the advantages of a quick response, whereas other components usually induce critical disturbance to the signals of exosomes in the spectra. The tag-based platforms are more selective than the label-free platforms, although tagging a probe with exosomes is also required. In the electrochemistry-based biosensors, an antibody-

modified electrode captures exosomes on its surface, and then the secondary antibody mediates the electrochemical reaction.

Conversely, the efficient isolation and collection of EVs from body fluids is also a challenging issue, as well as the measurement of EVs because of their small sizes and a wide distribution of sizes. Ultracentrifugation is a widely used isolation method for EVs despite the time-consuming process and low levels of recovery. Also, an expensive reagent and a large amount of sample are required. On the other hand, microfluidic devices have achieved high yields in the collection of EVs, but they require sophisticated fabrication techniques and complex pumping systems [11-14]. Compared with these separation methods, optical manipulation that is referred to either as laser trapping or optical tweezers is useful for collecting and manipulating small droplets [15-17] and vesicles [18,19].

Our previous research demonstrated that vesicles consisting of phospholipids would accumulate at the focal point of a laser beam [20]. When focusing a laser beam on the surface of a glass cuvette containing a suspension of the vesicles, the laser beam collected them at the focal point on the glass surface. Furthermore, we found that the addition of gold nanoparticles (AuNPs) significantly enhanced the collection speed of the vesicles via the interaction between the vesicles and the AuNPs. The mechanism for increased collection was based on the hydrophobic and electrostatic interactions between the vesicles and the AuNPs because the enhancement in optical force significantly depended on their surface charges [21]. A significant enhancement in the speed of the optical collection suggested that optical force would be potentially valuable for collecting small vesicles quickly in the presence of oppositely charged AuNPs.

Here, we describe enhancement of the optical collection of EVs via an interaction with AuNPs. An optical collection system was constructed to optically collect EVs from the culture media of cancer cells. The EVs were collected on an inner wall of a square capillary which was

filled with a cell culture medium. The addition of positively charged AuNPs significantly enhanced the collection efficiency of EVs because the membrane of EVs is comprised of phospholipids and membrane proteins [22] that produce negative charges similar to that of the cell surface [23]. In addition, the surface charge of the capillary wall also played an essential role in immobilizing EVs on the capillary wall. With a surface-modified capillary and positively charged AuNPs, EVs in a culture medium were collected optically.

Experimental

Materials

All reagents used in this study were of analytical grade without further purification. Deionized water was prepared by means of an Elix water purification system (Millipore Co. Ltd., Molsheim, France). Dulbecco's phosphate-buffered saline (DPBS) was purchased from Thermo Fisher Scientific. The exosome precipitation solution, ExoQuick-TC, was obtained from Funakoshi Co., Ltd. (Tokyo, Japan). Dipalmitoylphosphatidylcholine (DPPC) and 1,2-dipalmitoyl-*sn*-glycero-3-phosphate (PA) were obtained from Avanti Polar Lipids (Alabster, AL, USA). Sulfuric acid, acetic acid, and 30% hydrogen peroxide were obtained from Kanto Chemical (Tokyo, Japan). 3-Glycidyloxypropyltrimethoxysilane (GPTES) and 3-aminopropyltriethoxysilane (APTES) were purchased from Tokyo Chemical Industry (Tokyo, Japan). Other reagents were obtained from FUJIFILM Wako Pure Chemical Corporation (Osaka, Japan). Polyacrylamide gel (T=15%, e-PAGEL) was purchased from ATTO Corporation (Tokyo, Japan). A calibration kit with low molecular weight for use in electrophoresis was obtained from Cytiva (MA, USA). The methods used in the preparation of negatively charged vesicles and positively charged dimethylaminopyridine-coated gold nanoparticles (DMAP-AuNPs) are described in our previous paper [20,21]. Negatively charged vesicles were prepared by mixing DPPC and PA at a molar ratio of 10:1.

Apparatus

The size of the DMAP-AuNPs was estimated to be smaller than 15 nm according to the UV–Vis spectrum, as measured using a spectrophotometer (UV-2400PC, Shimadzu, Kyoto, Japan) [24], whereas a transmission electron microscope (TEM) image indicated that the sizes ranged from 1.1 to 13 nm (mean±standard deviation = 4.9±2.5, n = 500) (Supporting Information, Fig. S1). Electroosmotic mobilities in capillaries with different surface charges were measured using an absorbance detector (S-3702, Soma Optics, Tokyo, Japan) and a high-voltage power supply (HCZE 30-0.25, Matsusada Precision, Shiga, Japan). The electropherograms were recorded by a LabView program which read output voltages from the absorbance detector connected with an analog-to-digital converter.

Cell culture and isolation of EVs with a precipitation reagent

A HeLa cell line was obtained from the JCRB Cell Bank of the National Institutes of Biomedical Innovation, Health, and Nutrition (Osaka, Japan). Cells were cultured at 37 °C in Dulbecco's Modified Eagle Medium (Invitrogen, CA, USA) supplemented with 10%(v/v) calf bovine serum (Sigma Aldrich, MO, USA) and antibiotic-antimycotic, which contains penicillin G sodium salt, streptomycin sulfate, and amphotericin B (Invitrogen), prior to incubation under a 5% CO_2 atmosphere. The cells were cultured in 10-cm diameter petri dishes and split when the cell population was approximately 100% confluent.

To assess the enrichment factor of the optical collection method, a standard suspension of EVs was prepared by isolating EVs from a culture medium of HeLa cells according to the ExoQuick-TC protocol (System Biosciences, LLC, Palo Alto, CA), which is a commercially available precipitation reagent for exosomes. Initially, 10 mL of the culture medium was centrifuged at 2,580 × *g* for 15 min to remove cells and cell debris, and then 2 mL of ExoQuick-

TC was added to the supernatant of the culture medium. The mixture was let stand in a refrigerator at 4 °C for 12 h followed by centrifugation at 1,500 × g for 30 minutes at 4 °C, which resulted in a pellet of EVs at the bottom of the centrifuge tube. To prepare a 200-fold concentrated suspension of EVs, 50 µL of DPBS was added to the pellet.

Optical collection system

The inverted microscope system for optical collection of vesicles consists of an inverted microscope (Eclipse TE2000-S, Nikon, Tokyo, Japan) equipped with an objective lens (×40, N. A. 0.6), a CCD camera (Digital Sight 1000, Nikon), a notch filter (Techapec rugate notch filter, 532 nm, optical density >4, stock number #46−565, Edmund Optics, NJ) placed in front of the CCD camera to exclude scattered light from the laser beam, and a dichroic mirror (Di02-R514-25×36, Semrok, NY) to reflect the beam of a Nd:YAG laser (532 nm, maximum power, 3 W, Beamtech Optronics, Beijing, China), as reported previously [20]. A square capillary (i.d. and o.d.; 75×75 µm and 350×350 µm, Polymicro, CA) was cut into a 40-cm length, and its polyimide coating was removed to create a window 25 cm from one end of the capillary (Fig. 1). A laser beam was introduced into the inverted microscope via a dichroic mirror to focus on the capillary inner wall with the objective lens. The power of the laser passing through the trapping window of the capillary was adjusted to 44 mW. The inner wall of the capillary was observed using the CCD camera during the collection of vesicles to collect images and produce video. A sample solution containing either vesicles or EVs was injected into the capillary and continuously flowed at the flow rate of 5 µm s^{-1} to trap vesicles on the focal point of the laser beam on the capillary inner wall. The optical force was insufficient to trap the EVs at a flow rate higher than 10 µm s^{-1}. After turning the laser off, the trapped EVs were recovered in a microtube by injecting PBS from the injection end of the capillary.

Modification of the capillary inner wall

Capillary walls were modified via silane coupling [25] and piranha treatments [26]. For the silane coupling treatment, a capillary was pretreated by flushing 6 N HNO_3 for 3 h using a siphon method. After drying the capillary, GPTES- and APTES-modified capillaries were prepared by injecting a mixture of a silane-coupling reagent (GPTES or APTES) and methanol at a ratio of 1:1 into the capillary and letting stand overnight. For the piranha treatment, a capillary was filled with a mixture of concentrated H_2SO_4 and 30% H_2O_2 at a ratio of 1 : 3, and was let stand overnight. After the treatment, the capillary was washed with deionized water. The charges of the capillary walls were evaluated from the electroosmotic mobilities obtained by CE using an absorbance detector. Electroosmotic mobility was measured using cationic, anionic and neural markers (benzylamine, benzoic acid, and methanol). When the migration velocity of the neutral marker was too slow for detection, the electroosmotic flow was estimated by subtracting the effective electrophoretic mobility of cationic or anionic markers from the apparent electrophoretic mobility.

Characterization of EVs

The EVs collected by ExoQuick TC and optical force were characterized via nanoparticle tracking analysis (NTA), TEM, and sodium dodecyl sulfate-polyacrylamide gel electrophoresis (SDS-PAGE). The NTA and TEM analyses were performed using the charged analysis services of FUJIFILM Wako Pure Chemical Corporation and the Hanaichi UltraStructure Research Institute, Co., Ltd. (Okazaki, Japan). SDS-PAGE was carried out using a polyacrylamide gel of T=15%. Proteins separated in the gel were stained with coomassie brilliant blue.

Results and discussion

Size distribution and protein contents of EVs

To characterize the EVs employed in this study, we measured their size distribution, as shown in Fig. 2. The EVs collected by ExoQuick TC were smaller than 800 nm with a mean diameter of 190±8.3 nm (Fig. 2). The results suggest that the EVs collected by ExoQuick-TC cover a range of exosomes (50-150 nm) and microvesicles (100-1,000 nm). We speculated that the large particles would be aggregates of the small EVs. In fact, the TEM images found that the EVs collected by ExoQuick-TC somewhat contained aggregates as seen in the inset image of Fig. 2.

The proteins in the EVs collected by Exo-quick TC were separated by SDS-PAGE (Supporting Information, Fig. S2), which showed that the EVs contained several proteins that correspond to CD63 (~53 kD), CD40 (45~50 kD), CD9 (~25 kD), and CD81 (~26 kD) [27,28]. Therefore, the isolated EVs seem to contain microvesicles with exosomes.

Modification of the capillary wall

In a model experiment, the surface charges of model vesicles, AuNPs, and the capillary wall were controlled to assess the capturing performance. As shown in Table 1, the surface charges of the capillary walls and EVs were evaluated by their electroosmotic and effective electrophoretic mobilities (difference between the apparent electrophoretic mobility and the electroosomoptic mobility) measured via CE because they are directly proportional to their zeta potentials, i.e., their surface charges. In this study, positive electrophoretic mobilities were defined as the migration from the anode to the cathode in electrophoresis, i.e., the negative electrophoretic mobilities are the negative surface charges of EVs, and vice versa. However, it should be noted that a capillary surface has a negative charge when the electroosmotic mobility is positive under the definition. The electroosmotic mobility in the piranha-treated capillary is positive in the background electrolyte (BGE) at pH 8.6 and decreased slightly when DMAP-AuNPs were added to the BGE, which indicated a positive shift in the surface charge.

Conversely, an APTES-modified capillary showed a positively- charged surface as expected. Although a GPTES-modified capillary is expected to be neutral because of the epoxide or hydroxyl groups [29], the surface charge was negative in the BGE without addition of DMAP-AuNPs. When using the BGE containing 20 mM DMAP (no AuNPs), the electroosmotic mobility was slightly shifted to negative, which implies that DMAP reacted with and/or was adsorbed either by the epoxide or by the hydroxyl groups. It is interesting that the electroosmotic mobility of the GPTES-modified capillary became negative in the BGE with the addition of DMAP-AuNPs. This means that the DMAP-AuNPs reacted with and/or adsorbed to the functional groups of the capillary surface more efficiently on the GPTES-modified capillary than only DMAP, resulting in the formation of positively charged capillary walls. The electroosmotic mobility of the GPTES-modified capillary in the presence of DMAP-AuNPs was equal to that of the APTES-modified capillary, which suggests a positive surface charge. The EVs showed electrophoretic mobilities ranging from -2.1 to -1.7 in the absence of DMAP-AuNPs and from -1.2 to -1.0 in the presence of DMAP-AuNPs. These results imply that DMAP-AuNPs neutralize the negative charges of EVs via adsorption onto their surface, but the surface charges remain negative.

Because of the negative charge on the surface of the EVs listed in Table 1 and in the literature [23], negatively charged vesicles with a diameter of 1-μm were prepared with neutral DPPC and anionic PA for use as model vesicles. Two types of AuNPs, one coated with anionic citrate and the other with cationic DMAP, were examined to capture the negatively charged vesicles. When the capillary surface was charged negatively (piranha-treated capillary), citrate-AuNPs showed no collection of vesicles due to the electric repulsion between the citrate-AuNPs, vesicles, and capillary wall, as shown in Fig. 3 (a). On the other hand, the DMAP-AuNPs assisted in capturing the vesicles on the capillary wall when turning on the laser. The vesicles were immediately dispersed from the focal point, however, when the laser was turned off (Fig.

3 (b)). The phenomenon can be explained as follows. When DMAP-AuNPs are firmly bound to the vesicles the optical force that captures the vesicles is enhanced, whereas the electric repulsion between the vesicles and the capillary wall prevents immobilization of the vesicles on the capillary wall after the laser is turned off. The results shown in Fig. 3 (b) imply that the conjugate of an anionic vesicle and cationic DMAP-AuNPs remains negatively charged, which is consistent with the electrophoretic mobilities of EVs shown in Table 1.

Based on the results shown in Fig. 3 (b), a positively charged capillary was employed to enhance the electrostatic interaction of anionic vesicles with the capillary wall (Fig. 3 (c) and (d)). In Fig. 3 (c), the GPTES-modified capillary immobilizes the vesicles on its wall in the presence of citrate-AuNPs. However, the collection efficiency is significantly higher in the presence of DMAP-AuNPs (Fig. 3 (d) and Movie S1 in the Supporting Information) than when citrate-AuNPs are present (Fig. 3 (c)). Therefore, cationic DMAP-AuNPs enhance the optical force acting on the vesicles more efficiently than when anionic citrate-AuNPs are used. Observation of the collection process showed no large aggregates of EVs in the capillary even when adding AuNPs into the solution containing EVs.

The shape of AuNPs is also expected to influence the collection efficiency. The DMAP-AuNPs are spherical, as seen in the TEM image (Supporting Information, Fig. S1). The extinction band of the DMAP-AuNPs overlaps with the emission wavelength of the laser employed in this study so that the DMAP-AuNPs efficiently scatter the laser light. Conversely, many researchers have reported different shapes for AuNPs, such as nanorods and nanostars [30,31]. Because these materials have extinction maxima in the near-infrared region, they would be appropriate for near-infrared lasers. Therefore, spherical AuNPs are suitable for optical collection when using lasers emitting in the visible region.

Collection of EVs

According to the results shown in Fig. 3, a GPTES-modified capillary treated with DMAP-AuNPs (positively charged capillary) would enhance the collection efficiency of negatively charged EVs. Conversely, the concentration of DMAP-AuNPs and the laser power significantly influence the efficiency of EV collection on the capillary wall. Therefore, the collection efficiency of EVs at different levels of laser power was evaluated in the positively charged capillary using different concentrations of DMAP-AuNPs.

Similar to our previous report [20], the collection efficiency of EVs was evaluated using the area occupied by EVs when irradiating the laser light onto the capillary wall for 20 min. Table 2 shows how the collection efficiency depended on the concentration of DMAP-AuNPs when the sample solution containing EVs was prepared from a culture medium using ExoQuick-TC. The concentration ratios of DMAP-AuNPs to that of the EVs also are listed in Table 2. The area occupied by EVs was normalized by that obtained without AuNPs, as shown in Table 2. The area occupied by EVs gradually increased 45-fold at 0.2 nM to 73-fold at 2 nM, while 20 nM DMAP-AuNPs showed no collection of EVs. A high concentration of AuNPs inhibited the accumulation of EVs due to the strong extinction of the laser light via the scattering and absorption of the free AuNPs in the solution. At 2 nM DMAP-AuNPs, the concentration ratio is 4.8×10^5 which implies that the interactions between DMAP-AuNPs and EVs are relatively weak.

We varied the laser power and found it difficult to collect EVs at both low and high laser power. For example, 5 mW of laser power was too low and 100 mW generated bubbles that interfered with the collection of EVs (Fig. S3). At 17 and 44 mW, however, the laser beam efficiently captured the EVs with no significant differences (the relative areas occupied by EVs were 64.6 ± 6.65 and 72.6 ± 6.31). The results indicate that a laser power of 17 mW is sufficient to obtain the maximum yield of EVs while higher laser power is preferable to increase the

number of EVs trapped on the capillary surface. The bubble formation was attributed to AuNPs generated by heat due to the absorption of the laser light, which resulted in water evaporation.

The proposed model for the optical collection method is illustrated in Fig. 4. EVs bind with cationic DMAP-AuNPs mainly due to electrostatic interaction. The total charge of the resultant conjugate, however, is negative. Under laser beam irradiation, DMAP-AuNPs on the EVs enhance the scattering of the laser light, which intensifies the optical force and accelerates the movement of EVs in a direction perpendicular to the sample flow in the capillary. EVs then attach to the capillary wall because the surface charges of the two are opposite. Therefore, electrostatic interaction promotes retention of the EVs on the capillary wall even when the laser is turned off.

The collected amounts of EVs also depended on the concentration of EVs in the sample solution, as expected. When sample solutions with different concentrations were prepared using a suspension enriched using ExoQuick TC, the area occupied with EVs was expanded with increases in the EV concentration as shown in Fig. 5. It should be noted that the optical collection system successfully trapped and immobilized EVs on the capillary wall without preconcentration using ExoQuick TC. Therefore, the optical collection method permits the direct enrichment of EVs from culture media without preconcentration.

Conclusions

We have described a system for collecting EVs via an optical force that is enhanced by AuNPs. The collection system consists of an inverted microscope, a CCD camera, a laser for generating optical force, and a square capillary to flow a sample solution. The electric charges of the capillary wall and the AuNPs play important roles in the interactions of EVs with AuNPs and of EV-AuNP conjugates with the capillary wall. Optical collection requires fewer pretreatments, which is advantageous. The flow system with a square capillary facilitated

trapping, collection, and subsequent recovery of the EVs in a small volume. Although the number of EVs is insufficient for a standard analytical method, the speed of the optical collection is significantly accelerated by adding AuNPs. Therefore, when combined with a microfluidic system, the optical collection method will permit a microscale analysis of EVs that requires only several tens of μL for a sample. In summary, optical collection achieved a rapid, simple, and straightforward collection of EVs in culture media.

Declaration of Competing Interest

The authors declare that they have no known competing financial interests or personal relationships that could appear to influence the work reported in this paper.

Data Availability Statement

The datasets generated during and/or analyzed during the current study are available from the corresponding author on reasonable request.

Acknowledgments

This work was supported by JSPS KAKENHI Grant Numbers JP19H04675 and JP20H02766.

REFERENCES

1. J. Lötvall, A. F. Hill, F. Hochberg, E. I. Buzás, D. Di Vizio, C. Gardiner, Y. S. Gho, I. V. Kurochkin, S. Mathivanan, P. Quesenberry, S. Sahoo, H. Tahara, M. H. Wauben, K. W. Witwer, C. Théry, J. Extracell. Vesicles **3**, 26913 (2014).

2. M. Wu, Y. Ouyang, Z. Wang, R. Zhang, P. Huang, C. Chen, H. Li, P. Li, D. Quinn, M. Dao, S. Suresh, Y. Sadovsky, T. J. Huang, Proc. Natl. Acad. Sci. **114**, 10584 (2017).

3. J. Nilsson, J. Skog, A. Nordstrand, V. Baranov, L. Mincheva-Nilsson, X. O. Breakefield, A. Widmark, Br. J. Cancer **100**,1603 (2009).

4. E. J. Hoorn, T. Pisitkun, R. Zietse, P. Gross, J. Frokiaer, N. S. Wang, P. A. Gonzales, R. A. Star, M. A. Knepper, Nephrology **10**, 283 (2005).

5. A. Michael, S. D. Bajracharya, P. S. T. Yuen, H. Zhou, R. A. Star, G. G. Illei, I. Alevizos, Oral Dis. **16**, 34 (2010).

6. F. Song, C. Wang, C. Wang, J. Gao, H. Liu, Y. Zhang, L. Han, Anal. Chem. **93**, 4697 (2021).

7. M. He, J. Crow, M. Roth, Y. Zeng, A. K. Godwin, Lab Chip **14**, 3773(2014).

8. J. Park, M. Hwang, B. Choi, H. Jeong, J. Jung, H. K. Kim, S. Hong, J. Park, Y. Choi, Anal. Chem. **89**, 6695 (2017).

9. X. Doldan, P. Fagundez, A. Cayota, J. Laiz, J. P. Tosar, Anal. Chem. **88**, 10466 (2016).

10. D. Kwong Hong Tsang, T. J. Lieberthal, C. Watts, I. E. Dunlop, S. Ramadan, A. E. del Rio Hernandez, N. Klein, Sci. Rep. **9**, 13946 (2019).

11. S. Gholizadeh, M. Shehata Draz, M. Zarghooni, A. Sanati-Nezhad, S. Ghavami, H. Shafiee, M. Akbari, Biosens Bioelectron. **91**, 588 (2017).

12. F. Tian, C. Liu, L. Lin, Q. Chen, J. Sun, Trends Anal. Chem. **117**, 128 (2019).

13. W. Su, H. Li, W Chen, J. Qin, Trends Anal. Chem. **118**, 686 (2019).

14. T. L. Zhang, Z. Y. Hong, S. Y. Tang, W. Li, D. W. Inglis, Y. Hosokawa, Y. Yalikun, M. Li, Lab Chip **20**, 35 (2020).

15. M. Mitsunobu, S. Kobayashi, N. Takeyasu, T. Kaneta, Anal. Sci. **33**, 709 (2017).

16. Y.Tanaka, Y. Kohaku, S. Ishizaka, BUNSEKI KAGAKU **69**, 737 (2020).

17. R. Nakajima, A. Miura, S. Abe, N. Kitamura, Anal. Chem. **93**, 5218 (2021).

18. D. P. Cherney, J. C. Conboy, J. M. Harris, Anal. Chem. **75**, 6621 (2003).

19. D. P. Cherney, J. C. Conboy, J. M. Harris, Anal. Chem. **75**, 6621 (2003).

20. M. Kuboi, N. Takeyasu, T. Kaneta, ACS Omega **3**, 2527 (2018).

21. Y. Tani, T. Kaneta, Royal Soc. Open Sci. **6**, 190293 (2019).

22. T. Shimomura, R. Seino, K. Umezaki, A. Shimoda, T. Ezoe, M. Ishiyama, K. Akiyoshi, Bioconjugate Chem. **32**, 680 (2021).

23. M. Simons, G. Raposo, Curr. Opin. Cell Biol. **21**, 575 (2009).

24. W. Haiss, N. T. K. Thanh, J. Aveyard, D. G. Fernig, Anal. Chem. **79**, 4215 (2007).

25. D. G. Kurth, T. Bein, Langmuir **9**, 2965 (1993).

26. D. Maji, S. K. Lahiri, S. Das, Surf. Interface Anal. **44**, 62 (2012).

27. M. Chiba, M. Kimura, S. Asari, Oncol. Rep. **28**, 1551 (2012).

28. R. J. Noelle, J. A. Ledbetter, A. Aruffo, Immunol. Today, **13**, 431 (1992).

29. M. Mousavi, E. Fini, ACS Sustainable Chem. Eng. **8**, 3231 (2020).

30. S.-S. Chang, C.-W. Shih, C.-D. Chen, W.-C. Lai, C. R. C. Wang, Langmuir **15**, 701 (1999).

31. F. Hao, C. L. Nehl, J. H. Hafner, P. Nordlander, Nano Lett. **7**, 729 (2007).

Table 1 Electroosmotic mobilities in capillaries and electrophoretic mobilities of EVs

Capillary	Electroosmotic mobility/ 10^{-4} cm^2 s^{-1} V^{-1}	Electrophoretic mobility/ 10^{-4} cm^2 s^{-1} V^{-1}
Piranha-treated capillary		
BGE without AuNPs	3.7 ± 0.1	
BGE with DMAP-AuNPs	2.5 ± 0.4	
GPTES-modified capillary		
BGE without AuNPs	1.4 ± 0.2	
BGE with 20 mM free DMAP	0.55 ± 0.09	
BGE with DMAP-AuNPs	-3.6 ± 0.7	
APTES-modified capillary	-3.6± 0. 7	
EVs*		
Sample without AuNPs		-2.1 ~ -1.7
Sample with DMAP-AuNPs		-1.2 ~ -1.0

Background electrolyte (BGE), 50 mM Tris-borate (pH 8.6); electric potential; 10 kV (2-4 μA); effective length, 30 cm; total length, 50 cm; detection wavelength, 200 nm.

*The electrophoretic mobilities of EVs were measured using the BGE without DMAP-AuNPs.

Table 2 Dependence of the apparent collection efficiency on the concentration of DMAP-AuNPs

[AuNPs]/ nM	[AuNPs]/[EVs]	Relative area
0	0	1.00 ± 0.26
0.2	4.8×10^4	45.8 ± 3.94
2	4.8×10^5	72.6 ± 6.31
20	4.8×10^6	0

A 100-fold enriched EV suspension was diluted 10 times with DPBS; laser power, 44 mW; Relative area corresponds to the size of the aggregate formed by the collected EVs.

FIGURE LEGENDS

Figure 1 Experimental setup of the optical collection system.

Figure 2 NTA analysis and TEM images for the collected EVs using ExoQuick TC. Error bars indicate standard deviations (n=5).

Figure 3 Trapping of negatively charged vesicles by optical force in the presence of AuNPs. Conditions: (a) negatively charged capillary wall and anionic citrate-AuNPs, (b) negatively charged capillary wall and cationic DMAP-AuNPs, (c) positively charged capillary and anionic citrate-AuNPs, and (d) positively charged capillary and cationic DMAP-AuNPs. Vesicle size, 1 μm; laser power, 30 mW; collection time, 15 min; medium, DPBS.

Figure 4 Proposed model and protocol of the optical collection in the presence of DMAP-AuNPs.

Figure 5 The area occupied by EVs and its dependence on EV concentration.
(a) No enrichment; (b) 5-fold concentration, (c) 10-fold concentration, (d) 20-fold concentration. Conditions: laser power, 44 mW; irradiation time, 20 min; and, DMAP-AuNPs, 2 nM. Each sample was prepared via collection using the exosome precipitation reagent followed by suspension in DPBS.

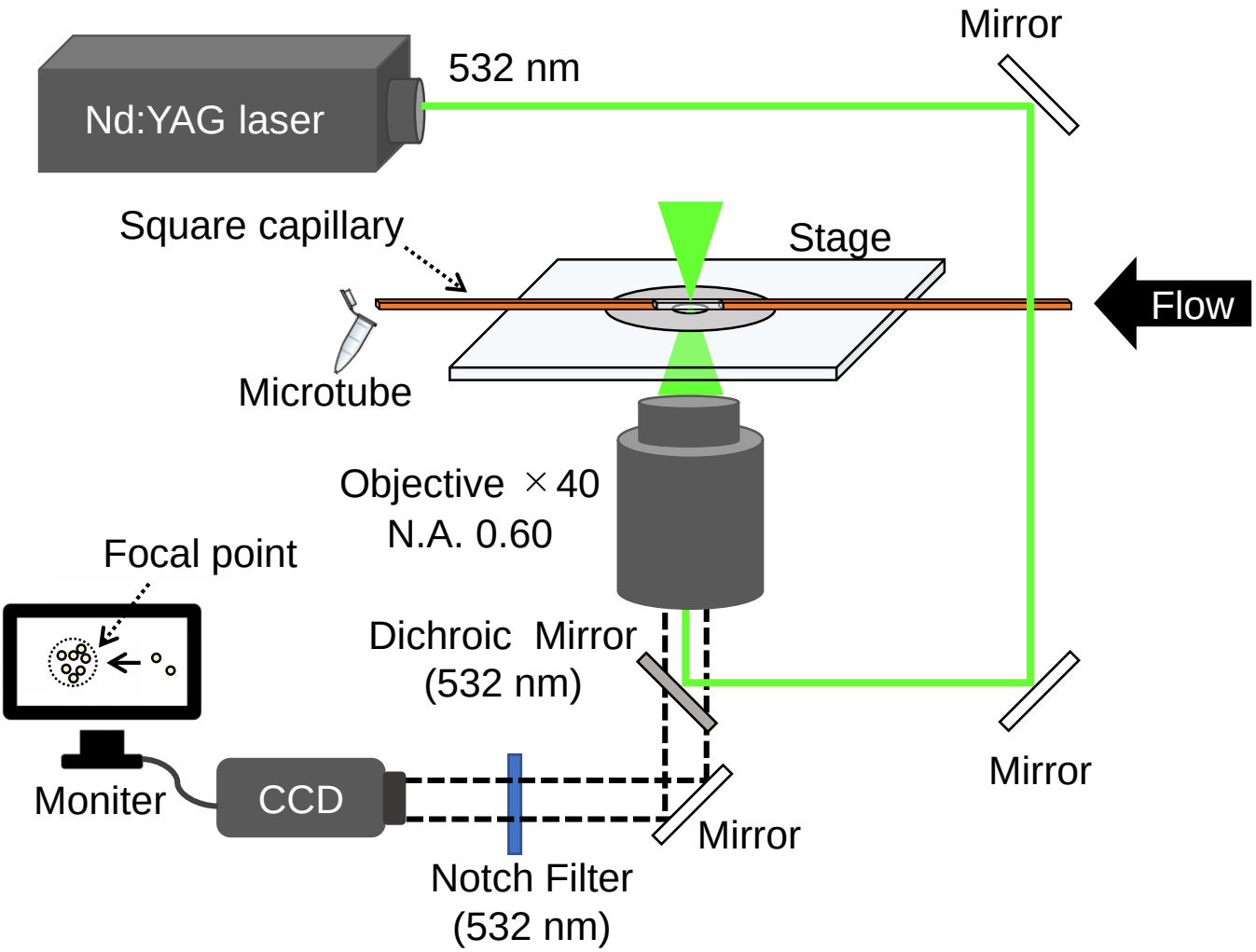
Mirror
Nd:YAG laser
532 nm
Square capillary
Stage
Flow
Microtube
Objective ×40
N.A. 0.60
Focal point
Dichroic Mirror
(532 nm)
Mirror
Moniter
CCD
Mirror
Notch Filter
(532 nm)

Figure 1

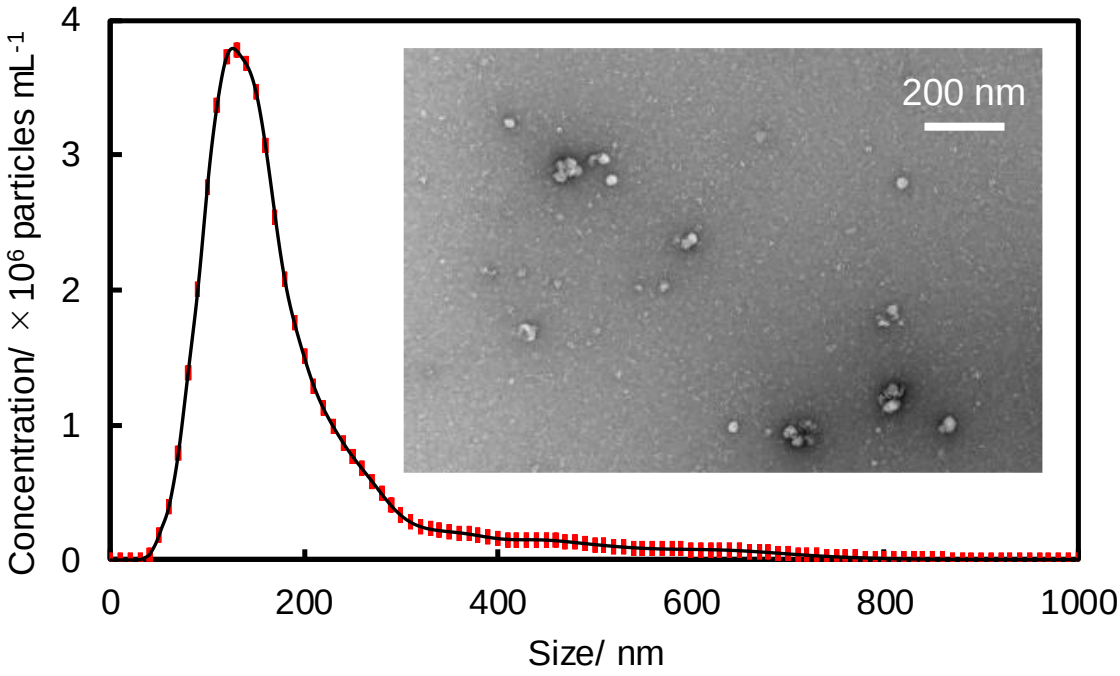
Concentration/ × 10^6 particles mL^-1
4
3
2
1
0
0
200
400
600
800
1000
Size/ nm
200 nm

Figure 2

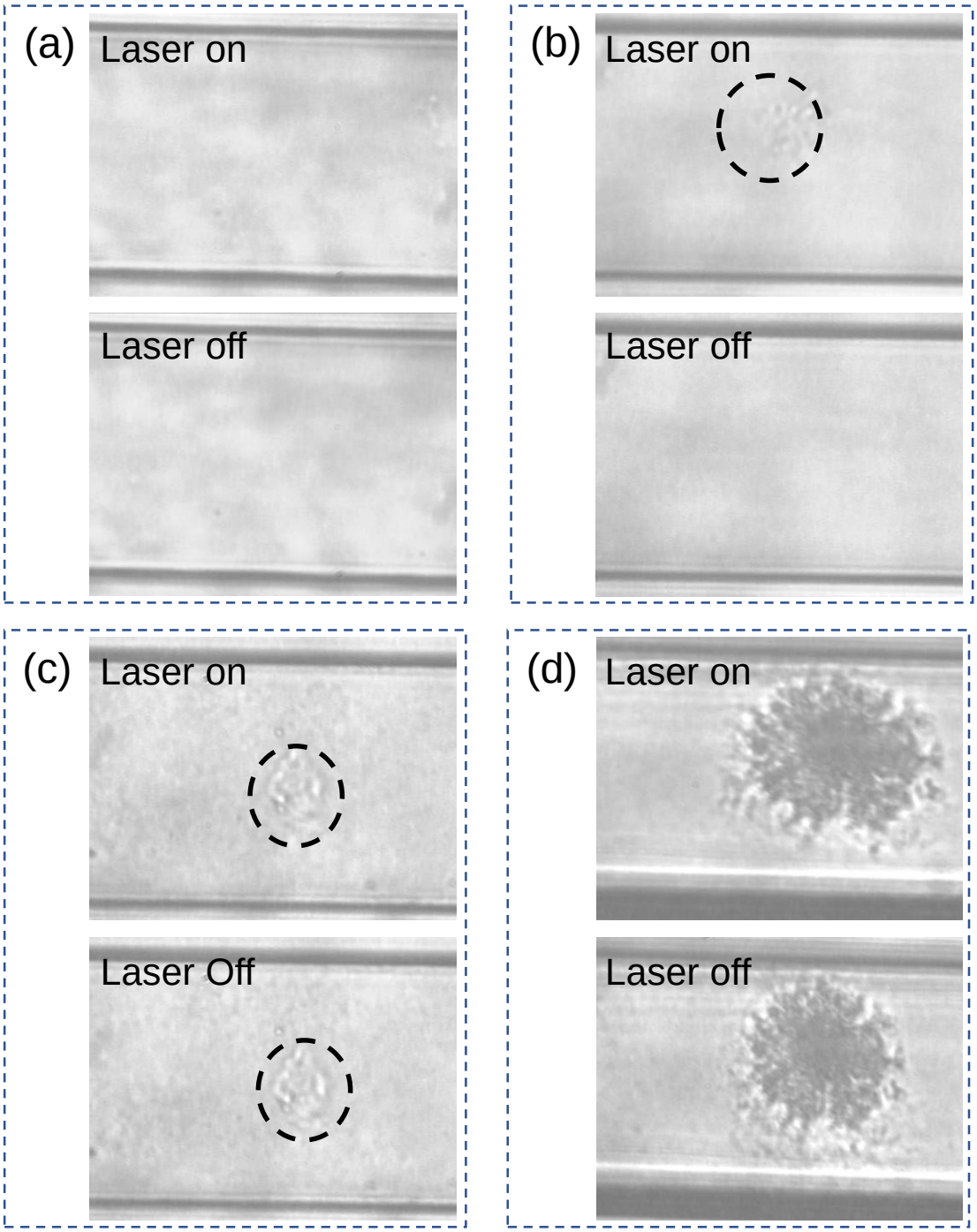
(a)
Laser on
Laser off
(b)
Laser on
Laser off
(c)
Laser on
Laser Off
(d)
Laser on
Laser off

Figure 3

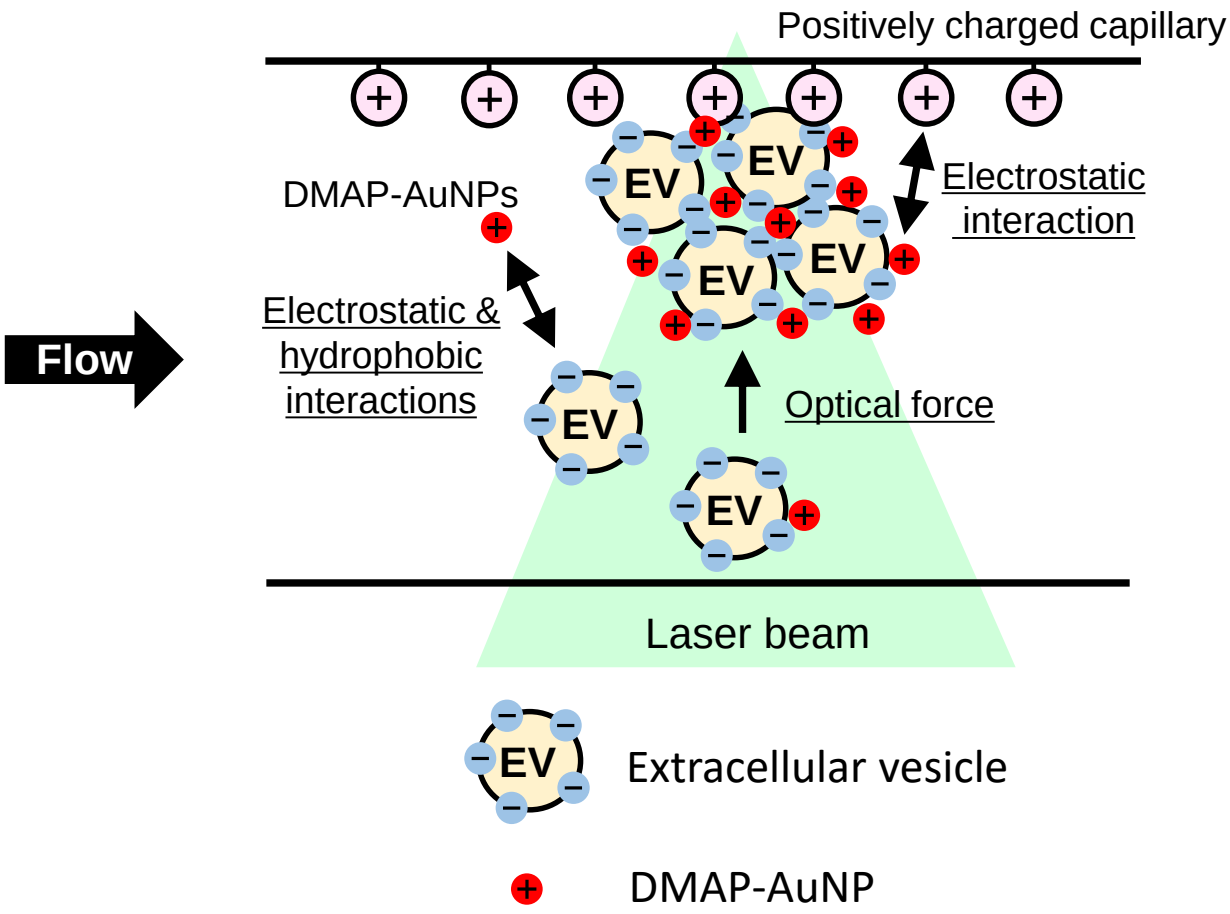
Positively charged capillary
DMAP-AuNPs
Electrostatic interaction
Electrostatic & hydrophobic interactions
Flow
Optical force
EV
Laser beam
Extracellular vesicle
DMAP-AuNP

Figure 4

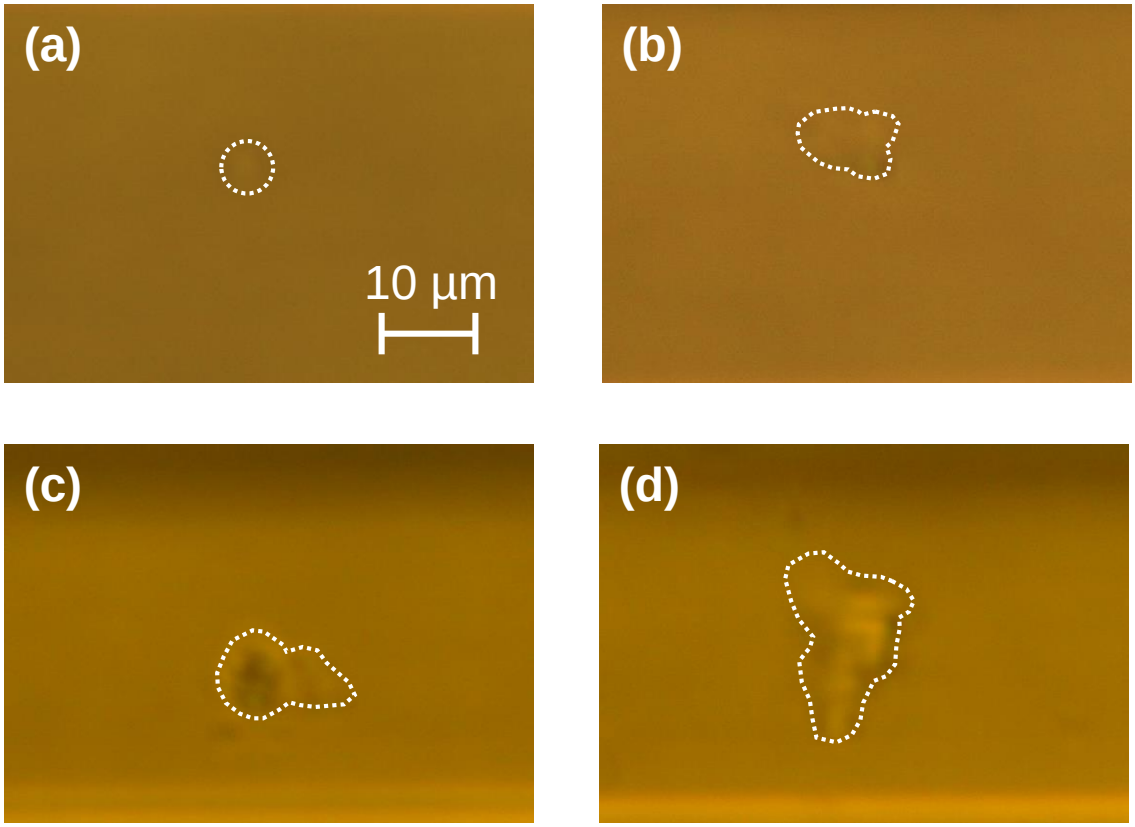

Figure 5

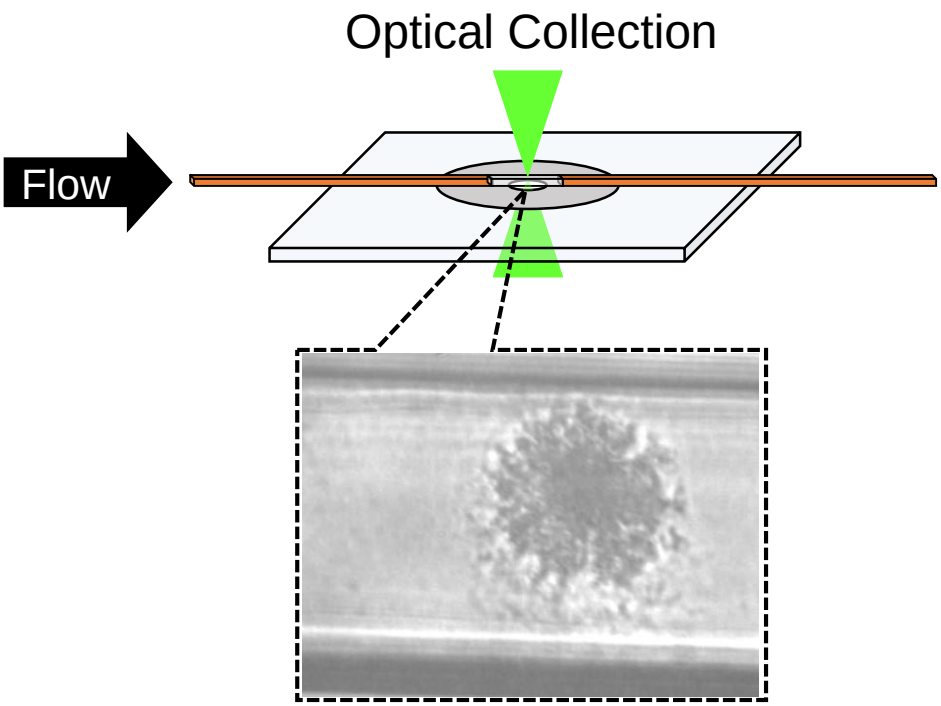
Optical Collection
Flow